Hydrol. Earth Syst. Sci. Discuss., https://doi.org/10.5194/hess-2018-452
Manuscript under review for journal Hydrol. Earth Syst. Sci.
Discussion started: 25 September 2018


Hydrology and Earth System Sciences
Discussions

# Reconstructing the Salgar 2015 Flash Flood Using Radar Retrievals and a Conceptual Modeling Framework: A Basis for a Better Flood Generating Mechanisms Discrimination

Nicolás Velásquez [1,2], Carlos D. Hoyos [1,2], Jaime I. Vélez [1], and Esneider Zapata [2]

[1]Universidad Nacional de Colombia, Sede Medellín, Facultad de Minas, Departamento de Geociencias y Medio Ambiente
[2]Sistema de Alerta Temprana de Medellín y el Valle de Aburrá (SIATA)

*Correspondence to:* Nicolás Velásquez (nvelasqg@unal.edu.co)

**Abstract.** Flash floods associated with severe precipitation events are highly destructive, often resulting in significant human and economic losses. Due to their nature, flash floods tend to occur in medium to small basins located within complex high mountainous regions. In the Colombian Andean region these basins are common, with the aggravating factor that the vulnerability is considerably high due to the presence of important human settlements frequently occupying floodplains and other flash-flood prone areas. During May 18 of 2015, severe rainfall generated a flash flood in the municipality of Salgar, in La Liboriana basin located in the northwestern Colombian Andes, resulting in more than 100 human casualties and significant economic losses. This work aims to reconstruct the 2015 La Liboriana flash flood to understand better the hydrological processes that took place during the event and to serve as a proof of concept for the development of a flash flood guidance low-cost tool when information is scarce. Radar QPE, satellite data, and post-event field visits are used to reconstruct the Salgar flash flood addressing the relationship between rainfall spatio-temporal structure, soil moisture, and runoff generation during successive rainfall events, using conceptual modeling framework including land-slide and hydraulic sub-models. The hydrological model includes the addition of virtual tracers to explore the role of runoff and subsurface flow, as well as the relative importance of convective and stratiform precipitation in flash flood generation. The assessment of the interactions between runoff, subsurface flow, and convective-stratiform rainfall allows a better understanding of the short-term hydrological mechanisms leading to the flash flood event. The overall methodology reproduces considerably well the magnitude and timing of La Liboriana flash flood discharge peak, as well as the areas of regional land-slide occurrence and flood spots location, with some limitations due to the available spatial scale of the digital elevation model. Simulation results

Hydrol. Earth Syst. Sci. Discuss., https://doi.org/10.5194/hess-2018-452
Manuscript under review for journal Hydrol. Earth Syst. Sci.
Discussion started: 25 September 2018


Hydrology and Earth System Sciences
Discussions
Open Access
EGU

indicate that the flash-flood and the regional land-slide features were strongly influenced by the antecedent rainfall associated with a northeasterly stratiform event that recharged the gravitational and capillary storages. The hydrologic simulation shows that the antecedent event set wet conditions in the entire basin before the occurrence of the flash flood event, governing the streamflow during the flash flood event. Evidence suggests that the spatial structure of the rainfall is at least as important as the geomorphological features of the basin regulating the generation of flash flood events. Results also suggest that the described model-based tool is useful for policy-makers not only for short-term decisions in the context of an early warning system but also as a planning resource for long-term risk management.

## 1 Introduction

Flash floods are regarded as one of the most destructive hydrological hazards resulting in considerable loss of human life and high costs due to infrastructure damages (Roux et al., 2011; Gruntfest and Handmer, 2001). Flash floods are usually described as rapidly rising water level events happening in streams and rivers, associated with short-term, very intense convective precipitation systems, or orographically forced rainfall events over highly saturated land surfaces and steep terrains (Šálek et al., 2006; Llasat et al., 2016; Douinot et al., 2016). Convective precipitation episodes often feature high intensities, short durations, and relatively reduced spatial coverage (Houze, 2004). Jonkman (2005), based on information from the International Disaster Database, maintained by the United States Office for Foreign Disaster Assistance and the Center for Research on the Epidemiology of Disasters in Brussels, shows that between 1975 and 2001 a total of 1816 worldwide freshwater flood events killed over 175,000 persons and affected more than 2.2 billion people. These events not only caused human and economic losses but also damages to ecosystems and loss of historical and cultural values. Among all different types of floods, Jonkman (2005) shows that flash floods result in the highest average mortality rate per event (3.62%), almost ten times larger than the mortality rate for river floods.

Several studies assess the role of rainfall, geomorphological features and soil conditions on flash floods occurrence from different points of view. Wu and Sidle (1995) highlight the role of the topography, ground cover, and groundwater in the occurrence of shallow landslides and associated debris flows. Merz and Blöschl (2003) highlighted the importance of understanding the physical processes giving rise to floods of a certain probability of occurrence and proposed a framework, from a catchment perspective, for identifying causative mechanisms of inundations and the viability for a large number of episodes and basins. Given the critical role of precipitation, some authors follow a climatological approximation to assess the recurrence of flash floods in particular regions

Hydrol. Earth Syst. Sci. Discuss., https://doi.org/10.5194/hess-2018-452
Manuscript under review for journal Hydrol. Earth Syst. Sci.
Discussion started: 25 September 2018


Hydrology and Earth System Sciences
Discussions

and study the different atmospheric causative mechanisms. These studies have evidenced the need to incorporate global and regional climatological conditions and variability in local risk reduction. For example, Kahana et al. (2002) examined the extent to which floods in the Negev Desert are the outcome of distinct climatological synoptic-scale features finding that about 80% of the events can be linked to distinct synoptic types characterized by the prevailing atmospheric conditions days prior the flood events. Schumacher and Johnson (2005) studied extreme rain events associated with flash flooding in the United States over a 3-yr period using the national radar reflectivity composite data are to examine the structure and evolution of each extreme rain events. Schumacher and Johnson (2005) found that 65% of the total number of episodes are associated with mesoscale convective systems (MCSs), with two recurrent patterns of organization: the existence of training convective elements and the generation of quasi-stationary areas of convection with stratiform rainfall downstream. Fragoso et al. (2012) analyzed storm characteristics and required rainfall conditions for flash flood occurrence at Madeira (Portugal), and their results suggest an essential role of global climate patterns (North Atlantic Oscillation -NAO- forcing) and also local forcing (orographic features) in the triggering of such events. Piper et al. (2016) examined the critical elements of flash flood triggering storms following a statistical approach, finding an essential role of stationary convective cores. Gochis et al. (2015) studied the great Colorado flood of 2013, documenting not only the meteorological conditions but also the climatological ones responsible for producing the observed widespread destruction, associating them with the potential for sustaining a blocking ridge over the Canadian Rockies and a slow-moving, cutoff, upper-level cyclonic circulation to its south over the western United States. Implicitly, all the studies mentioned and all the others available in the peer-reviewed literature point to the need for local and regional quality spatio-temporal rainfall data. Berne and Krajewski (2013) highlight the need to incorporate high-resolution weather radar information, even with some limitations, in flash flood hydrology.

Different authors have shown that antecedent soil moisture significantly influences the occurrence and behavior of flash floods. Rodriguez-Blanco et al. (2012) analyzed fifty-four flash flood episodes in Spain and determined that antecedent conditions are a vital point in runoff production. Castillo et al. (2003), using a modeling approach, highlighted the role of antecedent moisture conditions in flash flood occurrence associating them with different kinds of storm events. Aronica et al. (2012) used spatial and statistical analysis to reconstruct landslides and deposits, finding a connection between flash flood occurrence and soil moisture antecedent conditions. Tramblay et al. (2012) showed better flash flood model performance when using remotely sensed soil moisture data as initial conditions in a hydrological modeling study. Other authors have tried to understand the governing processes of flash floods from the geological formation of the basin (Adamovic et al., 2016; Vannier et al., 2016).

Hydrol. Earth Syst. Sci. Discuss., https://doi.org/10.5194/hess-2018-452
Manuscript under review for journal Hydrol. Earth Syst. Sci.
Discussion started: 25 September 2018




Due to the rapid nature of flash floods, they are more likely to occur in small and steep basins (Younis et al., 2008), highlighting the need for the availability of detailed temporal scale precipitation data (Norbiato et al., 2008) and high-resolution terrain information. Watersheds prone to these events are usually located in rural mountainous areas with poor gauge information (rain and level). The utilization of radar data to study flash flood generating storms is vital for understanding and forecasting these events (National Research Council 1996). One of the most critical challenges associated with flash floods is their simulation and prediction (Yamanaka and Ma, 2017; Borga et al., 2011; Marra et al., 2017). The fact that flash floods are more prone in small basins increases their intrinsic physical and measurement uncertainty (Wagener et al., 2007), difficulting their prediction (Hardy et al., 2016; Ruiz-Villanueva et al., 2013). Many authors have assessed the influence of hills and stream slopes and evidence suggest the slopes of the hills are significantly more important for flash floods occurrence and magnitude than the stream slope (, eds.; Šálek et al., 2006; Roux et al., 2011; Yatheendradas et al., 2008).

Arguably one of the most meaningful applications of quantitative precipitation estimation (QPE) from a societal point of view is its use to improve flash flood forecasting. The use of weather radar QPE products in flash flood applications could potentially offset, in part, the lack of in-situ precipitation products in small poorly gauged basins and become an important stepping stone for improving the state-of-the-art understanding of flash flood processes such as orographically enhanced extreme rainfall events and runoff generation (Creutin and Borga, 2003a). However, in some cases, there still exist limitations associated with the spatial resolution of radar retrievals (Šálek et al., 2006; Hardy et al., 2016). Nevertheless, several modern approaches involving radar information, in-situ precipitation data, model approximations and merging algorithms are promising (Braud et al., 2016).

The topography of Colombia is characterized by three branches of the Andes crossing the country south-to-north, generating a mixture of landscapes from high snow-capped mountains, vast highland plateaus, deep canyons to wide valleys, making some regions highly prone to flash flood occurrence. The likelihood of flash flood occurrence in Colombia is also high due to the spatio-temporal behavior of the Intertropical Convergence Zone, and the direction of the near-surface moist air flow leading to orographic enhancement of convective cores (Poveda et al., 2007). In the last decade, there have been several widespread and localized flash flood events in Colombia associated with climatological features and with the local intensification of rainfall events. The 2010-2011 La Niña event alone triggered 1233 flooding events and 778 mass removal processes, with more than 3 million people affected and damages estimated by the "Comisión Económica para América Latina y el Caribe " in more than 6.5 billion US dollars. After this widespread disaster, several localized events have occurred in the country with devastating consequences.

Hydrol. Earth Syst. Sci. Discuss., https://doi.org/10.5194/hess-2018-452
Manuscript under review for journal Hydrol. Earth Syst. Sci.
Discussion started: 25 September 2018




Between May 15th and May 18th, 2015, several storms took place over La Liboriana basin located in the municipality of Salgar, in the department of Antioquia (Colombia). By 2015, the population of Salgar was estimated at 17400 persons, 8800 residing in the urban area. La Liboriana is a small tropical basin ($56km^2$) located in the western range (Cordillera Occidental) of the Colombian Andes. During the night of May 17th, between 02:00 and 09:00 A.M. (local time), a precipitation event covered almost all the basin (hereafter referred to as event 1). Twenty hours later, between 23:00 P.M of May 17 and 02:00 A.M. of May 18 two successive extreme convective systems occurred over the basin with the maximum intensity in the upper hills (event 2). Event 1 corresponds mainly to a stratiform event, covering almost all the basin area and with an average precipitation accumulation of 47 $mm$. Event 2 accumulated, averaging over the basin, around 38 $mm$, however over the upper watershed the accumulation exceeded 180 $mm$. The occurrence of these successive rainfall events resulted in a flash flood that took more than 100 human lives and affected several buildings and critical infrastructure. The total investment for the reconstruction of Salgar´s infrastructure and the psychosocial attention of the community is estimated at 36.000 million Colombian pesos (approximately 12,5 million dollars considering 2018 exchange rate), which corresponds to three times the annual income of the municipality. Figure 1 shows an example of infrastructure damage as a result of the flash flood event, and satellite images of the basin's main channel before and after the flash flood, showing considerable river margins and bed erosion.

La Liboriana basin flash flood is a typical case of prediction in ungauged basins (PUB) (Sivapalan et al., 2016; Seibert and Beven, 2009; Beven, 2007; Bonell et al., 2006; Yamanaka and Ma, 2017). In this case, there are no local records of soils or land use and the local hydro-meteorological data is scarce or non-existent and certainly not available in real time. Due to the lack of data, La Liboriana case imposes a challenge for flash flood prediction and modeling. According to Blöschl et al. (2012), there are three methods for using models in PUB cases. The first strategy is to obtain the required model parameters from historical basin behavior and the morphological characteristics of the basin. This strategy often leads to low model performance (Duan et al., 2006). The second approach is to inherit the hydrological calibration from a gauged neighboring watershed, which in this case does not exist. The third method is to parameterize the model based on proxy variables, such as hydraulic information obtained during field recognition. In the case of the 2015 La Liboriana basin flash flood, there are no previous historical streamflow records, nor records from a neighboring watershed.

The present work aims to reconstruct the 2015 La Liboriana flash flood, not only to understand better the hydrological processes that took place during the event but also to serve as a proof of concept that hopefully leads to the development of a flash flood guidance low-cost tool based on the scarce information existent. Such a tool should be useful for decision-makers not only for short-term decisions in the context of an early warning system but also as a planning resource for long-term

Hydrol. Earth Syst. Sci. Discuss., https://doi.org/10.5194/hess-2018-452
Manuscript under review for journal Hydrol. Earth Syst. Sci.
Discussion started: 25 September 2018


Hydrology and Earth System Sciences
Discussions
Open Access
EGU


a) Aerial photograph before the event (2012).


b) Aerial photograph taken after the event (2015-05).

**Figure 1.** Example of infrastructure damage as a result of the La Liboriana May 18 of 2015 flash flood event. a) Aerial photograph before the event (2012) taken during a mission of the Department of Antioquia´s Government, and b) satellite image after the event (2015-05). The images show the destruction of most houses in that particular community, a bridge over La Liboriana, and the main road. The images also present changes in the delineation of the main channel as well as considerable erosion in the river margins.

risk management. In particular, this work uses information derived from radar QPE, satellite data, and post-event field visits to reconstruct the Salgar flash flood event. Also, this study addresses two broad hydrological issues. The first issue consists in exploring the relationship between rainfall spatio-temporal structure (Llasat et al., 2016; Fragoso et al., 2012), soil moisture and runoff generation (Penna et al., 2011; Tramblay et al., 2012; Garambois et al., 2013) during the successive rainfall events. The second issue consists in proposing a simplified hydrological modeling scheme including land-slide and hydraulic sub-models to detect and anticipate potential flash flood events.

The methodology followed in this study makes use of a conceptual modeling framework that includes a hydrological model, a shallow land-slide sub-model, and a hydraulic sub-model. The hy-

Hydrol. Earth Syst. Sci. Discuss., https://doi.org/10.5194/hess-2018-452
Manuscript under review for journal Hydrol. Earth Syst. Sci.
Discussion started: 25 September 2018


Hydrology and Earth System Sciences
Discussions

drological model, based on the work by Vélez (2001) and Francés et al. (2007), simulates different hydrological processes as independent but interacting storages. The shallow landslide sub-model follows the formulation described in (Aristizábal et al., 2016). The hydraulic sub-model corresponds to a low-cost 1D model (hereafter referred to as HydroFlash) that assumes infinite sediment supply and estimates the cross-sectional filled area at all time steps. The hydrological model includes the addition of virtual tracers to explore separately the role of runoff and subsurface flow, as well as the relative importance of convective and stratiform precipitation in flash flood generation. The convective and stratiform classification follows the methodology proposed by Houze et al. (2015) and Steiner et al. (1995). The assessment of the interactions between runoff, subsurface flow, and convective-stratiform rainfall allows a better understanding of the short-term hydrological mechanisms leading to the flash flood event. The model is parameterized using field information from a river cross-section located at the entrance of the urban area of Salgar. A comparison between the results from both sub-models and the observed landslides scars and flooded spots helps to evaluate the overall skill of the proposed methodology.

The document is structured as follows. Section 2 describes in more detail the region of study, La Liboriana basin, including geomorphological and climatological characteristics of the basin as well as the information sources used in this study. Section 3 presents a description of the overall methodology and the model used for the reconstruction of the 2015 La Liboriana flash flood event, including flow separation, shallow landslide parameterization, and the proposed hydraulic model. Section 4 describes the main results of the study, including model parameterization and validation. Section 4 also includes a discussion on the role of the rainfall structure in the flash flood reconstruction and presents results from the land-slide and inundation sub-models. Finally, the conclusions are presented in section 6.

## 2 Data and Area of Study

The urban area of Salgar municipality is located near the outlet of La Liboriana basin, a small (56 $km^2$) tropical watershed located in the westernmost range of Colombia's Andes (Figure 2). La Liboriana basin joins El Barroso river basin and both drain to Cauca river. The availability of the ALOS-PALSAR Digital Elevation Model (DEM) (ASF, 2011), with a resolution of about 12.7 $m$, allows estimating the fundamental geomorphological features. The average slope of La Liboriana is 57.6 %, and the basin longitude and perimeter are 13.5 $km$ and 57.8 $km$, respectively. The Strahler-Horton order of the principal stream is 5, and the longitude and slope of the principal stream are 18.1 $km$ and 8.1 % respectively. The highest elevation of the watershed (Cerro Plateado) reaches 3609 meters above sea level (m.a.s.l), while the outlet of the basin is at 1316 m.a.s.l.. The longitudinal profile (see Figure 3) exhibits considerable steepness in the upper basin. The 99th slope percentile

Hydrol. Earth Syst. Sci. Discuss., https://doi.org/10.5194/hess-2018-452
Manuscript under review for journal Hydrol. Earth Syst. Sci.
Discussion started: 25 September 2018


Hydrology and Earth System Sciences
Discussions
Open Access
EGU

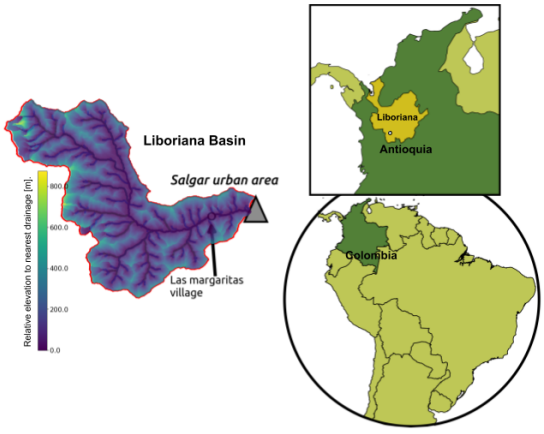


**Figure 2.** Geographical context of Liboriana basin, located in Colombia, in the Department of Antioquia. The color bar represents the Height Above the Nearest Drainage (HAND). Low HAND values correspond to areas prone to flooding.

of order 1 streams is 78%. For streams order 2, 3, 4, and 5 the 99th slope percentile are 61, 27, 18 y 11%, respectively. These features are typical of Andean mountainous basins. The hypsometric curve shows considerable elevation changes for a cumulative area below 33% (see blue line in Figure 3). Geomorphologically, this kind of watershed is prone to the occurrence of flash floods.

At the sub-basin scale, La Liboriana exhibits a vast range of slopes and altitude differences. Figure 2 shows the Height Above the Nearest Drainage -HAND- model (Rennó et al., 2008) for La Liboriana. The HAND calculates the relative difference between cell $i$ and its nearest streamflow cell $j$. La Liboriana HAND exhibits values between 500 and 800$m$. Near the outlet of the basin, over the banks, there are values close to 0 m. High HAND values at the upper region of the watershed often denote areas of high potential energy, with increased sediment production and frequent shallow landslides occurrence. Banks with low HAND values are more susceptible to flooding and tend to correspond to areas prone to extensive damages caused by extreme events. While the elevation differences described in Figure 2 are typical of the region, the social challenges lie in the high vulnerability of the Salgar given the location of the main urban settlement.

Vegetation and land use vary considerably within the basin. In the upper La Liboriana basin, there are crop fields and tropical forests; a portion of the watershed is considered a national park. Hillslopes near the divide do not evidence significant anthropic intervention most likely due steepness of the slopes in this region. Down the hills and at the bottom of the valley there are coffee plantations (the primary economic activity of the region) and pastures. The watershed exhibits grazing areas and

Hydrol. Earth Syst. Sci. Discuss., https://doi.org/10.5194/hess-2018-452
Manuscript under review for journal Hydrol. Earth Syst. Sci.
Discussion started: 25 September 2018


Hydrology and Earth System Sciences
Discussions
Open Access
EGU

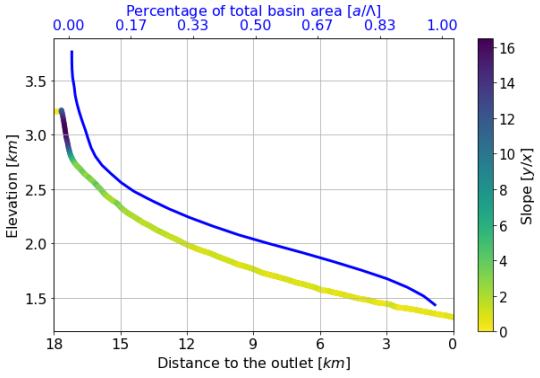


**Figure 3.** Longitudinal profile of the principal stream (colored line) from the upper part of the basin to its outlet at the entrance of the urban area, hypsometric curve of the drainage basin (blue line).

**Table 1.** Description of the soils in the region (Osorio, 2008).

| Type | Slope | Depth [$m$] | Retention | Permeability |
|---|---|---|---|---|
| **Class III** | 12-25 | 0.6 | Mean | Mean |
| **Class IV** | <12 | 0.6 | Low | High |
| **Class VI** | 25-30 | 1.0 | Mean | Mean |
| **Class VII** | 30-50 | 0.3 | Too Low | Slow |
| **Class VIII** | >50 | 0.2 | Too Low | Slow |

urban development near the river banks .

The Andean Colombian region tends to present well-developed soils of different textures with a predominance of limes and clays. One of the challenges for hydrological modeling and risk management in the country is that soils are not well mapped; national soil cartography is usually available in 1:400.000 scale. At this scale, the municipality of Salgar, including La Liboriana basin, corresponds to only one soil texture. The only available information corresponds to descriptions by regional authorities. Osorio (2008) describe La Liboriana soils as well-drained with poor retention capacity. Organic material is predominant in the first layer and clay loam soil within the second one. The depth of the soil is hillslope dependent, varying between 20$cm$ and 1$m$ (Osorio, 2008). Table 1 provides a summary of soil characteristics for five different categories, all as a function of slope. Each soil category has a corresponding depth and a qualitative description of permeability and retention.

A field campaign few days after the flash flood event was instrumental in obtaining cross-section geometry along the main channel, including at the outlet of the basin. The cross-section has a rectangular shape, and it is 4.6$m$ wide and has a height of 5$m$ for a total area of about 23$m^2$. A visual

Hydrol. Earth Syst. Sci. Discuss., https://doi.org/10.5194/hess-2018-452
Manuscript under review for journal Hydrol. Earth Syst. Sci.
Discussion started: 25 September 2018


Hydrology and Earth System Sciences
Discussions
Open Access
EGU


**Figure 4.** Channel cross-section shown an example of flooded infrastructure after the flash flood event. The section shows mud marks on the walls with heights varying between 0.5 and 1.2 $m$. These mud stains are evident in buildings located 4-5 $m$ away from the channel. The photograph also shows the width of the channel and the total estimated depth during the flash flood.

inspection of the flooded infrastructure around this section reveals the presence of mud marks on the walls with heights varying between 0.5 and 1.2 $m$. These mud stains are evident in buildings located 4-5 $m$ away from the channel (see Figure 4). The area of the section plus the flooded area during the event was estimated to be approximately 37 $m^2$. Assuming flow speeds between 5 and 6 $m/s$, the total discharge required to generate the observed flash flood vary between 185 and 222 $m^3/s$. In this work, the soil information and the field campaign are used to parametrize a hydrological model. Field campaign estimates and satellite imagery are central to validate the results from the proposed hydrological model.

The reconstruction of the 2015 Salgar flash flood event following a hydrological modeling strategy uses a radar-based QPE technique developed by Sepúlveda and Hoyos (2018) to obtain spatiotemporal precipitation maps over the basin. A detailed description of the estimation, as well as the overall meteorological conditions that led to the La Liboriana extreme event, are described in a companion paper (Hoyos et al. 2018). The QPE technique uses retrievals from a C-band polarimetric Doppler weather radar operated by the Sistema de Alertas Tempranas de Medellín y del Valle de Aburra (SIATA, is a local early warning system from a neighboring region, www.siata.gov.co) and it is located at 100$km$ away from the basin. The radar has an optimal optimum range of 120 $km$ radius and a maximum operational range of 240 $km$. The radar operating strategy allows obtaining precipitation information every 5$min$ and the spatial resolution is about 128 $m$. The sensor is a C-band polarimetric Doppler weather radar operated by the Sistema de Alertas Tempranas de Medellín y del Valle de Aburra (SIATA, a local early warning system from a neighboring region, www.siata.gov.co) and located at 100$km$ away from the basin. The radar has an optimal optimum range of 120 $km$ radius and a maximum operational range of 240 $km$. The radar operating strategy allows obtaining

Hydrol. Earth Syst. Sci. Discuss., https://doi.org/10.5194/hess-2018-452
Manuscript under review for journal Hydrol. Earth Syst. Sci.
Discussion started: 25 September 2018


Hydrology and Earth System Sciences
Discussions

precipitation information every $5min$ and with a spatial resolution is about 128 $m$.

## 3 Methodology

The overall methodology followed in the reconstruction of the 2015 Salgar flash flood, is presented in an illustrative diagram in Figure 5. The availability of radar-based QPE and a detailed DEM allows the use of a modeling framework based on the distributed hydrological model described in Vélez (2001) and Francés et al. (2007) with important modifications (left column in Figure 5). The hydrological model simulates different hydrological processes as independent, but interacting storages. The model distributes processes by cells; in each cell, five tanks represent the hydrological processes including capillary (tank 1), gravitational (tank 2), runoff (tank 3), baseflow (tank 4) and channel storage (tank 5). The state of each tank varies in function of vertical and lateral flows as shown in the diagram, where the storage is represented by $S_i$, the vertical input by $D_i$ which in turns depends on $R_i$. $E_i$ represents the downstream connection between cells, except for tank 1, where $E_1$ represents the evaporation rate. Vertical flows are only time dependent, while lateral flows could also depend on the actual state of the tank (kinematic approximation).

The model modifications fall in four different categories: (i) the direct use of radar QPE as a source of rainfall information, (ii) the implementation of virtual tracers for surface and subsurface discharge as well as for convective and stratiform water tracing, (iii) the development of two modules for hazard assessment, and (iv) the enforcement of a maximum gravitational storage ($H_g$) to allow Hortonian runoff (return flow from $S_3$ to $S_2$). The virtual tracers are critical to explore separately the relative role of superficial runoff and subsurface flow, as well as the relative importance of convective and stratiform precipitation in flash flood generation. The convective and stratiform classification follows the methodology proposed by Houze et al. (2015) and Steiner et al. (1995). The implementation of convective and stratiform rainfall separation and virtual tracers are presented in the top two right panels of the illustrative diagram in Figure 5. The hydrological model allows hazard assessment by coupling a shallow landslide model (Aristizábal et al., 2016), and a new low-cost 1d hydraulic flash flood model referred to here as **HydroFlash**. The implementation of the shallow landslides model and HydroFlash are schematized in the bottom two right panels of the illustrative diagram in Figure 5.

For the technically inclined reader, the hydrological model and sub-models are written in Fortran 90, and the interface to the model, pre-process, and post-process tools are in python 2.7. The Fortran code is warped to python using **f2py** (Peterson, 2009) and it is publicly available under the Water-

Hydrol. Earth Syst. Sci. Discuss., https://doi.org/10.5194/hess-2018-452
Manuscript under review for journal Hydrol. Earth Syst. Sci.
Discussion started: 25 September 2018


Hydrology and Earth System Sciences
Discussions
Open Access
EGU

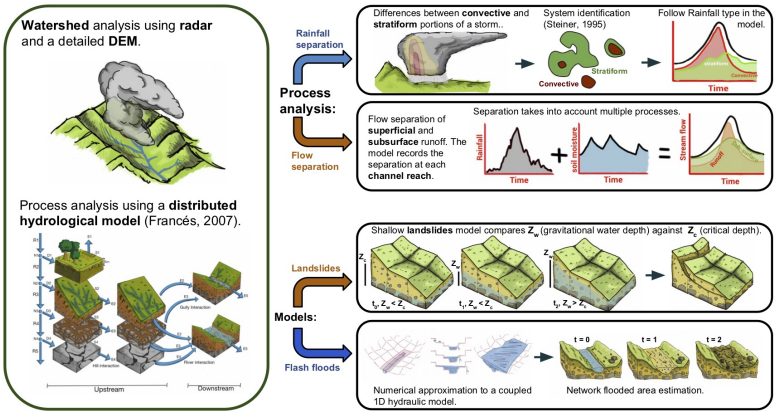


**Figure 5.** Illustrative diagram of the methodology followed in the present study. The left column represents the availability of radar-based QPE and a detailed DEM as the basis of the modeling framework and the mains aspects of the distributed hydrological model used. In each cell five tanks represent the hydrological processes including capillary (tank 1), gravitational (tank 2), runoff (tank 3), baseflow (tank 4) and channel storage (tank 5). The state of each tank varies in function of vertical and lateral flows as shown in the diagram, where the storage is represented by $S_i$, the vertical input by $D_i$ which in turns depends on $R_i$. $E_i$ represents the downstream connection between cells, and evaporation. The implementation of convective and stratiform rainfall separation and virtual tracers are presented in the top two right panels. The implementation of the shallow landslides model and HydroFlash are schematized in the bottom two right panels.

shed Modelling Framework **WMF** in a web repository (**GitHub**).

### 3.1 Virtual Tracers

Virtual tracers are implemented into the model to discriminate streamflow source in superficial runoff and subsurface flow and to assess the portion of streamflow from convective rainfall and stratiform precipitation, recording at each time stem and each cell the source of water. The model archives the results of the virtual tracing algorithm at the outlet of the basin and at each reach allowing the study of the role of flows from different nature during extreme events at different spatial scales to get more insights about the soil-driven flow regulation. The soil texture and composition could play diverging roles during extreme events. The soil could work as a porous medium in which the water travels fast, making the subsurface flow an essential part of the hydrograph, or on the other hand, its saturation could lead to a decrease in infiltration rates and a potential increase of surface runoff generation.

The flow separation module operates in tanks 2 (runoff storage) and 3 (subsurface storage). The module marks water once it reaches any of those two tanks and the runoff-subsurface flow percent-

Hydrol. Earth Syst. Sci. Discuss., https://doi.org/10.5194/hess-2018-452
Manuscript under review for journal Hydrol. Earth Syst. Sci.
Discussion started: 25 September 2018




age are taken into account once the water enters tank 5 (the channel). At this point, the scheme assumes that the water in the channel is well mixed, implying that the flow percentage is constant until a new inflow enters the channel.

Both spatial and temporal rainfall variability influence the hydrograph Shope (2016). Stratiform rain cells cover large areas and are related to long duration hydrographs with low peak flow. On the other hand, convective rainfall cells cover limited areas and are related to short duration hydrographs with high peak flows. Stratiform rainfall tends to recharge the basin, while convective tends to increase runoff generation and the formation of the hydrograph. In the literature, these associations have often been more qualitative than quantitative (Creutin and Borga, 2003b; Šálek et al., 2006; Borga et al., 2014).

Rainfall from radar reflectivity fields is classified into stratiform and convective using the Steiner et al. (1995) approach before the implementation of the rainfall tracer. At each time step, the model takes into account the total rainfall, assuming that at each particular cell the precipitation is either entirely convective or entirely stratiform. This assumption could lead to estimation errors at basins represented by coarse cells (low DEM resolution) where convective and stratiform precipitation are likely to coexist. In the present study the spatial resolution of the DEM is $12.7m$, higher than the resolution of the radar retrievals (about $125m$), so the potential convective and stratiform rainfall concurrence is very low, and it could not be identified using the Steiner et al. (1995) approach. Once within the model, rainfall separation follows the methodology proposed for flow type separation.

### 3.2 Hazards Assessment

During the 2015 La Liboriana flash flood event, two central processes took place. Shallow landslides occurred in the upper basin, and a flash flood generated flooding, and human and infrastructure losses.

#### Shallow landslides sub-model

The shallow landslides submodel coupled to the hydrological model is proposed by Aristizábal et al.. The model conceptualizes the stability of a cell based on the concept of an infinite slope described by the geomorphological and soil properties of the cell. The model classifies cells into three groups: unconditionally stable, conditionally stable and unconditionally unstable. Figure 6 describes the variables of the model and the balance of forces considered. Three parameters determine stability of each cell: (i) residual soil thickness water table $Z_{i,min}$ estimated as in equation (1), (ii) the maximum soil depth at which a particular soil remains stable $Z_{i,max}$ estimated as in equation (2), and (iii) the max-

Hydrol. Earth Syst. Sci. Discuss., https://doi.org/10.5194/hess-2018-452
Manuscript under review for journal Hydrol. Earth Syst. Sci.
Discussion started: 25 September 2018


Hydrology and Earth System Sciences
Discussions
Open Access
EGU

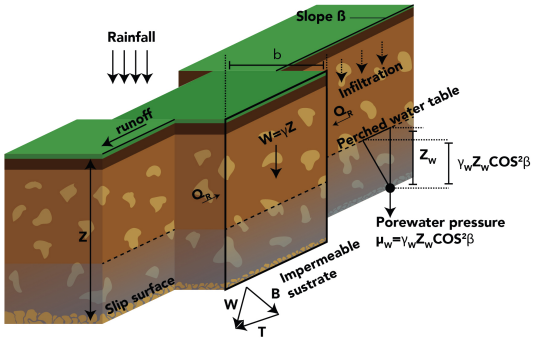


**Figure 6.** The geotechnical conceptual model. $\gamma$ is the soil bulk density, $\gamma_w$ is the water density, $Z_w$ is the saturated soil thickness above the slip surface, $Z$ is the soil thickness measured vertically, $\beta$ is the gradient of the hillslope. And $Q_L$ and $Q_R$ are the resultant forces on the sides of the slice. Figure and description are adapted from Aristizábal et al. (2016).

imum slope at which the soil remains stable $\beta_{i,0}$ estimated as in equation (3).

$$Z_{i,min} = \frac{C'}{\gamma_w cos^2\beta tan\phi + \gamma cos^2\beta(tan\beta - tan\phi)} \tag{1}$$

$$Z_{i,max} = \frac{C'}{\gamma cos^2\beta(tan\beta - tan\phi)} \tag{2}$$

$$\beta_{i,0} = tan^{-1}\left[tan\phi\left(1 - \frac{\gamma_w}{\gamma}\right)\right] \tag{3}$$

The model assess conditionally stable cells in function of their perched water table for each cell ($Z_{i,w}$, equation (4)) and the critical satured depth ($Z_{i,c}$). Slope failure occurs when $Z_{i,w}$ is greater than $Z_{i,c}$. $Z_{i,c}$ is obtain using equation (5).

$$Z_{i,w}(t) = \frac{S_{3,t}}{W_c - W_{fc}} \tag{4}$$

$$Z_{i,c} = \frac{\gamma}{\gamma_w} Z\left(1 - \frac{tan\beta}{tan\phi}\right) + \frac{C'}{\gamma_w cos^2\beta tan\phi} \tag{5}$$

where $S_{3,i}$ represents gravitational storage, $Ws$ and $W_{fc}$ the soil saturation and field capacity respectively, $\gamma$ represents soil density, $\phi$ is the soil stability angle, $C'$ the soil cohesion and $\beta$ the cell slope.

Hydrol. Earth Syst. Sci. Discuss., https://doi.org/10.5194/hess-2018-452
Manuscript under review for journal Hydrol. Earth Syst. Sci.
Discussion started: 25 September 2018




**Flash flood submodel (HydroFlash)**

It is common to use complex hydraulic 2D and 3D models, such as Iber (Cea and Blade, 2015) or HEC (Gibson et al., 2010) for flood spots identification. This kind of modeling requires detailed information about the terrain and river bathymetry and are usually implemented for a particular river cross section due to the high information demand and high computational costs, precluding the operational implementation of 2D and 3D methodologies in regions with scarce resources. Also, this traditional hydraulic methodology tends to analyze only some network elements, overlooking the complexity of the basin. In this work, we introduce a low-cost 1D hydraulic model for flash flood simulation referred to as HydroFlash. The model extracts the cross-profile from the DEM for each cell considered part of the network, estimating flood spots at each network cell during execution time.

The model requires hydraulic parameters for all network cells to determine flash-flooding spots. Channel width is estimated using the Leopold (1953) approach $W_i = 3.26\overline{Q_i}^{0.469}$. Channel slope ($S_{i,0}$) is obtained as the mean value of the slopes that correspond to the cells of a hydrological reach. The characteristic particle diameter $D_{i,50}$ is assumed equal to 0.138 and constant. The cross-section ($C_s$) is obtained from the DEM, for every network cell, perpendicular to the flow direction of the cell ($D_{i,8}$).

For each time step $t$ and for each stream cell, equation (6) determines the height of the water table $Y_i(t)$ using the simulated streamflow $Q_{i,sim}$(t) and flow velocity $v_{i,sim}(t)$. The model calculates the friction velocity ($v_{fr,i}$) using $Y_i$ as in equation (7) derived from Keulegan and Rouse equations (Takahashi, 1991). Equations (8) and (9) allow the estimation of the concentration ($c_i(t)$) and constitutive coefficients ($r_i$), respectively. The stream flow plus estimated sediments and rubble is estimated according to equation (10).

$$Y_i = \frac{Q_{i,sim}}{v_{i,sim} w_i} \tag{6}$$

$$v_{fr,i} = \frac{v_{i,sim}}{5.75 log\left(\frac{Y_i}{D_{i,50}}\right) + 6.25} \tag{7}$$

$$c_i = C_{max}(0.06 Y_i)^{\frac{0.2}{v_{fr,i}}} \tag{8}$$

$$r_i = \left(\frac{1}{D_{i,50}}\right)\left(\left(\frac{9.81}{0.0128}(c_i + (1 - c_i)\right)\left(\frac{\gamma_w}{\gamma_{sed}}\right)\right)^{0.5}\left(\frac{C_{max}}{c_i}\right)^{(1/3)-1.0} \tag{9}$$

Hydrol. Earth Syst. Sci. Discuss., https://doi.org/10.5194/hess-2018-452
Manuscript under review for journal Hydrol. Earth Syst. Sci.
Discussion started: 25 September 2018




405

$$Q_{i,sed} = Q_{i,sim}\frac{1+c_i}{1-c_i} \tag{10}$$

assuming infinite sediment and rubble supply, $Q_{i,sed}$ is the maximum stream flow for the section. To determine the flooded area, an equivalent $Y_{i,sed}$ must be found in order to obtain an stream flow ($\hat{Q}_{i,sed}$) (equation (11)) that equals $Q_{i,sed}$. The estimation of $Y_{i,sed}$ is an iterative process . The
410 model obtains the flooded area ($A_{i,sed}$) based on $Y_{i,sed}$ and equation (12).

$$\hat{Q}_{i,sed} = \left(\frac{2}{5}\right) r_i (j\Delta y_{i,sed})^{\frac{3}{2}} S_{i,0} 0.5 \hat{A}_{i,sed} \tag{11}$$

$$\hat{A}_{i,sed} = \Delta x \sum_{j=1}^{N} (Y_{i,sed} + \Delta y_{i,sed}) - C_{j,s} \tag{12}$$

415 Resulting flood maps might evidence the presence of small isolated flood spots and discontinuities at flood spots where flow direction changes from orthogonal to diagonal or vice-versa. We included two post-processing steps to correct these issues by (i) using an image processing erosion algorithm to remove the small isolated flood spots. The erosion is performed once with a 3x3 kernel, and (ii) to solve the flow direction discontinuities, each flooded cell seeks to flood its eight neighboring cells. A
420 neighbor cell is also flooded if the altitude of the original flooded cell plus the flood depth is higher than its altitude.

### 3.3 Hydrological runoff scheme modification

Horizontal flow equations could be either linear or potential, as shown in equation (13). In the mod-
425 ified hydrological model, $\beta$ and $\alpha$ are estimated by the user and then set into the model.

$$v_{tank}(t) = \beta A(t)^{\alpha} \tag{13}$$

Non-linear equations in lateral flows could result in a better representation of processes at high resolutions (Beven, 1981; Kirkby and Chorley, 1967). A non-linear approximation to runoff is pre-
430 sented in equation (14). This approximation is a modification of Manning's formula for flow in gullies. According to Foster G.R. (1984), the values of $\varepsilon$ and $e_1$ are 0.5 and 0.64, respectively. The non-linear equation (15) corresponds to an adaptation of Kubota and Sivapalan (1995) formula for subsurface runoff.

$$v_2 = \frac{\varepsilon}{n} S_0^{1/2} A_2(t)^{(2/3)e_1} \tag{14}$$

Hydrol. Earth Syst. Sci. Discuss., https://doi.org/10.5194/hess-2018-452
Manuscript under review for journal Hydrol. Earth Syst. Sci.
Discussion started: 25 September 2018




$$v_3 = \frac{K_s S_o^2}{(b+1)A_g^b} A_3(t)^b \tag{15}$$

Where $k_s$ is the saturated hydraulic conductivity, and $b$ is dependent on the soil type, and it is assumed equal to 2. $A_g$ is the equivalent cross-section area to the maximum gravitational storage ($H_g$). There is also return flow from tank 3 to tank 2 when $S_3 = H_g$, representing runoff generation by saturation.

The equations describe the momentum of a kinematic wave approximation. In both cases, velocity depends on the tank storage. These relations could be summarized by the equation (13), that could be solved numerically coupled with a mass balance equation (16). This equation takes into account the storage at each time step ($S_{tank}(t)$), the longitude of the element ($\Delta x$), the time step size ($\Delta t$), and the speed estimated for the flow in the time step ($v_{tank}(t)$). Equation (16) is related to equation (13) through the velocity term ($v_{tank}$) and the cross-sectional area ($A$). The solution to $v_{tank}$ and $A$ is obtained through an iterative scheme. The total outflow from the tank is calculated using equation (17).

$$A(t) = \frac{S_{tank}(t)}{\Delta x + v_{tank}(t)\Delta t} \tag{16}$$

$$E_{tank}(t) = A(t) v_{tank}(t) \Delta t \tag{17}$$

## 4 Results

The primary results of the present study include the reconstruction of the 2015 Salgar flash flood, the assessment of the importance of soil moisture in the hydrologic response of the basin, and the evaluation of the relative role of stratiform and convective precipitation cores in the generation of the observed extreme event. This section is based on the results from the analysis of the hydrological simulation, as well as shallow landslides and flash floods occurrence and simulation.

Figure 7a presents the temporal evolution of the convective-stratiform rainfall partitioning during both Events 1 and 2. The main difference between both events is the timing of the convective versus stratiform participation within each case. Event 1 started as a stratiform precipitation event moving from the southwest, from the Department of Chocó to the Department of Antioquia across western-most Andes mountain range. Chochó is the rainiest department in Colombia, and one of the wettest places on Earth, due to the inflow of moisture from the Pacific Ocean and the orientation of the Andes mountain range (Poveda and Mesa, 2000; Mapes et al., 2003). After 3 hours of stratiform rainfall,

Hydrol. Earth Syst. Sci. Discuss., https://doi.org/10.5194/hess-2018-452
Manuscript under review for journal Hydrol. Earth Syst. Sci.
Discussion started: 25 September 2018


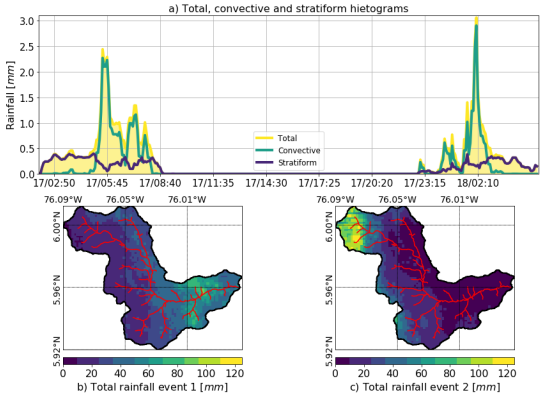


**Figure 7.** a) Temporal evolution of the convective-stratiform rainfall partitioning during both Events 1 and 2. The figure shows the total rainfall (yellow), and the convective (blue) and stratiform (green) portions integrated over La Liboriana basin. b) and c) Spatial distribution of the cumulative rainfall during Events 1 and 2 over La Liboriana basin.

training convective cores move over La Liboriana basin generating intense precipitation peaks during 2.5 hours. It is important to note that these cores did not strengthen within La Liboriana basin; these systems formed and intensified over the western hills of Farallones de Citará draining to the Department of Chocó towards Atrato river. The latter is not a minor fact because once the convective system move with a northeast direction, the maximum intensity cores do not fall over the steepest hills of La Liboriana basin but rather near the basin outlet where the slopes are considerably flatter. Figure 7b shows the spatial distribution cumulative rainfall during Event 1, corresponding to a basin-average precipitation accumulation of 47 $mm$,with the maximum precipitation located towards the bottom third of the basin. Event 2, on the other hand, started as a thunderstorm training event with two convective cores moving from the southeast followed by remaining stratiform precipitation. Even though the average cumulative rainfall over the basin was 9 $mm$ less than during Event 1, this event is characterized by orographic intensification within the basin leading to a more heterogeneous spatial distribution and with the highest cumulative precipitation in the steepest portion of the basin (see Figure 7b). Event 2 spatial distribution and highly localized observed intensities most likely led to the flash-flooding episode, as it is explored in the remainder of this section.

Figure 8a presents the results of the hydrological simulation at the outlet of the basin. The model simulation is set to reach a base flow of 3 $m^3/s$, a value that corresponds to the discharge measurements during field campaigns days and weeks after the flash flood event and during dry spells. The simulation shows that Event 1 generates a hydrograph with a peak flow of $Q_{max}$ = 160 $m^3/s$ that did not result in casualties or infrastructure losses, but set wet conditions in the entire basin

Hydrol. Earth Syst. Sci. Discuss., https://doi.org/10.5194/hess-2018-452
Manuscript under review for journal Hydrol. Earth Syst. Sci.
Discussion started: 25 September 2018


Hydrology and Earth System Sciences
Discussions
Open Access
EGU

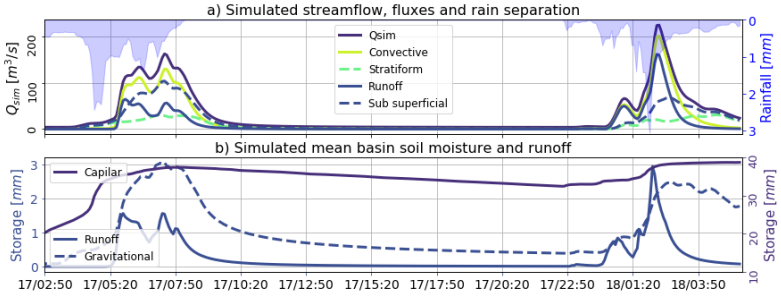


**Figure 8.** Summary of the Results from the hydrological simulation. a) Simulated streamflow, runoff and subsuperficial flow separation and convective-stratiform generated discharge discrimination. b) Mean runoff, gravitational, and capillary storages during the simulation period.

before the occurrence of Event 2 (see the purple line in Figure 8b). Additionally, it is clear from the simulation that during the flash flood event the two successive convective cores over the same region (training convection) generated a peak flow of $Q_{max}$ =220 $m^3/s$, value that is in the upper range of the estimated streamflow based on a posteriori field evidence (185-222 $m^3/s$). Figure 8a also presents the runoff and subsurface flow separation as well as the convective-stratiform generated discharge discrimination. The evidence during Event 2 suggests the convective rainfall fraction dominates hydrograph formation. In both events, convective (stratiform) precipitation appears to be closely related to runoff (subsurface flow). On the other hand, subsurface flow is more important in magnitude than runoff describing Event 1, while runoff is more relevant for Event 2.

Figure 8b presents capillary storage (purple), as well as runoff (continuous blue) and gravitational (dashed blue) storage temporal variability. As expected, runoff storage is only non-zero during the storm duration, while gravitational storage increases considerably during rain events, followed by a slow recession. There is an increment of basin-wide capillary storage during Event 1, remaining considerably high the time leading to the occurrence of Event 2.

In this study, we propose a graphical method to assess the soil-rainfall-discharge coupling holistically. The first step is to classify all the cells within the watershed in a predetermined number of groups according to their localization and the distance to the outlet. The aim is to establish a coherent and robust spatial discretization, thus allowing to summarize the concurrent spatio-temporal variability of the different processes in 2D diagrams. Figure 9 presents an example of the spatial structure of cell grouping for La Liboriana basin using 10 (left) and 50 (right) groups.

Figure 10 presents the proposed 2D diagrams obtained for the simulation of the La Liboriana basin flash flood using a spatial discretization with 50 groups. Figure 10a includes the evolution of

Hydrol. Earth Syst. Sci. Discuss., https://doi.org/10.5194/hess-2018-452
Manuscript under review for journal Hydrol. Earth Syst. Sci.
Discussion started: 25 September 2018


Hydrology and Earth System Sciences
Discussions
Open Access
EGU

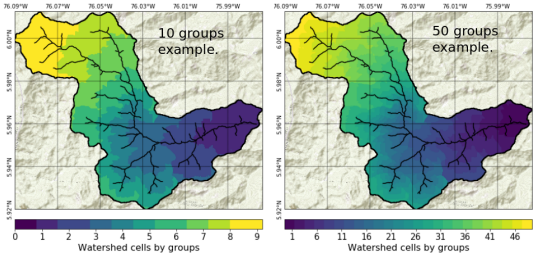


**Figure 9.** Example of watershed grouping as a function of distance to the outlet for La Liboriana basin. The left panel corresponds to clustering using ten different groups, and the right panel shows the 50-groups categorization used in the present study.

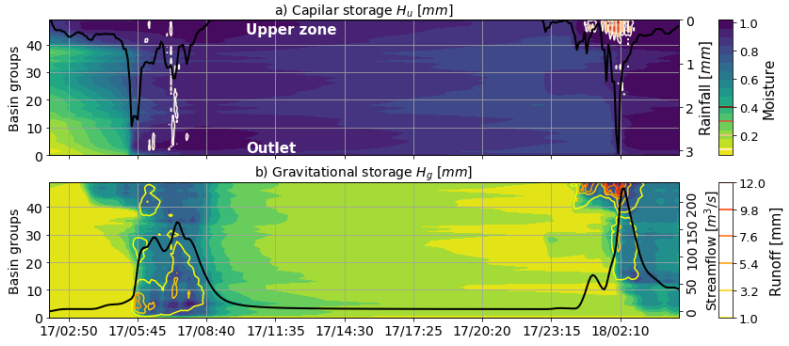


**Figure 10.** Spatiotemporal analysis of Events 1 and 2. a) Simulated capillary moisture (filled green-to-blue contours) and returned flow occurrence (white to red isolines). The black line represents the average rainfall over the basin. b) Simulated gravitational moisture (filled green-to-blue contours) and runoff (yellow-to-red isolines). The black line represents streamflow at the outlet of the basin. The green-to-blue color bar serves as a reference for capillary moisture and gravitational water content.

the average rainfall over the basin (black line), and the spatio-temporal evolution of capillary storage (filled isolines) and return flow (colored isolines from white to red) by groups. For the analysis, it is relevant to highlight that higher numbered groups are located away from the outlet of the basin and correspond in this case to considerably steeper slopes. Figure 10b presents the evolution of streamflow at the outlet of the basin (black line) as well as the gravitational storage (filled isolines) and runoff (colored isolines) spatio-temporal evolution.

It is well known that temporal variability of rainfall intensity plays an important role in hydrograph structure. During Event 1 rainfall accumulated over the basin at a relatively stable rate (Figure 11a). On the other hand, Event 2 presents a significant increase in rainfall rate in the second half of

Hydrol. Earth Syst. Sci. Discuss., https://doi.org/10.5194/hess-2018-452
Manuscript under review for journal Hydrol. Earth Syst. Sci.
Discussion started: 25 September 2018


Hydrology and Earth System Sciences
Discussions

the life cycle (Figure 11b). This change in precipitation intensity is associated with a considerable intensification of the training convective cores due to orographic effects. Events 1 and 2 also exhibit differences in the elapsed time between rainfall occurrence and streamflow increment given the relative timing of stratiform versus convective rainfall (see the gray band in Figure 11a and b). For Event 1, the median elapsed time between rainfall and streamflow ($Et_{p50}$) is 1.12 hours while for Event 2 $Et_{p50}$ is 0.79 hours. The median elapsed time between the convective portion and the streamflow ($Etc_{p50}$) in Event 1 is 0.75 and 0.46 in Event 2. The minimum value of the convective elapsed time $Etc_{min}$ also descends from 0.42 to 0.25 hours. On the other hand, there is an increase of median elapsed time between stratiform rainfall and streamflow ($Ets_{p50}$) from 1.21 to 1.83 hours. In Event 2, the convective rainfall and the runoff show a similar evolution, denoting a strong influence of the convective portion (Figure 11b).

As mentioned before, average rainfall accumulation over the basin for Events 1 and 2 is $47mm$ and $38mm$, respectively. During Event 1 (2), convective (stratiform) average accumulations are 28 (23) and 17 (14) $mm$, respectively (Figure 12a and b). The maximum rainfall intensities are relatively similar with $150mm/h$ and $180mm/h$ for Events 1 and 2, respectively. Despite this, Event 1 does not trigger a flash flood event. The overall evidence suggests that the discriminating factor between both events does not lie in the portions of convective or stratiform rainfall but rather in their spatial distribution.

Figures 12a and b, and Figures 12c and d show the convective and stratiform cumulative rainfall, and the spatially-averaged convective and stratiform rainfall, both as a function of sub-basin reach, respectively. Figures 12a and b show that while Event 1 exhibit similar convective and stratiform rainfall accumulation for different watershed scales, Event 2 shows a more significant cumulative contribution of convective rainfall than of stratiform precipitation. Convective rainfall tends to cover less area, and at the same time present a spatio-temporal erratic behavior (Steiner et al., 1995; Houze, 1989). Figures 12c and d provide evidence that convective rainfall present higher variations at small sub-basins than for a larger-order basin. During Event 2, convective accumulation reaches higher values for small and medium sub-basins. Convective rainfall occurrence at the upper sub-basins has significant implications due to geomorphological conditions associated to zero-order sub-basins (Sidle et al., 2018). Figure 13 presents Pearson correlations coefficients between the convective and stratiform hydrograph portions and the runoff and subsurface flow. According to this, convective and stratiform rainfall exhibit a weaker relationship with the flow characteristics at small scales (under $5km^2$). This is likely to be associated with increasing variability of rainfall and hydrograph formation at small scales (Ayalew et al., 2014). Correlations tend to grow with increasing area, indicating stabilization of the hydrograph formation. Additionally, subsurface flow presents higher correlations during Event 1, while correlations with runoff are higher for Event 2, highlighting the most impor-

Hydrol. Earth Syst. Sci. Discuss., https://doi.org/10.5194/hess-2018-452
Manuscript under review for journal Hydrol. Earth Syst. Sci.
Discussion started: 25 September 2018


Hydrology and Earth System Sciences
Discussions
Open Access
EGU

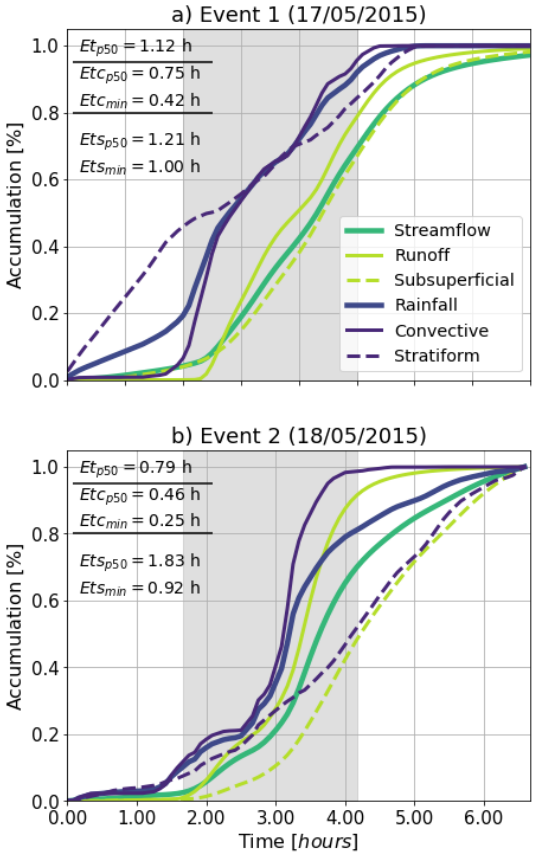


**Figure 11.** Accumulated rainfall and streamflow for a) Event 1 and b) Event 2. The accumulation is expressed in percentage respect to the total value in each case. Median elapsed time and minimum elapsed time () are estimated between total ($Et_{p50}$, $Et_{min}$), convective ($Etc_{p50}$, $Etc_{min}$), and stratiform ($Ets_{p50}$, $Ets_{min}$) rainfall and the runoff portion of the streamflow. Gray bands correspond to the periods for elapsed time estimation.

560 tant process in each case. The relevance of subsurface flow is likely due to the rainfall characteristics during Event 1, with homogeneous rainfall intensity and high rate of basin recharge (see Figure 8b). On the other hand, saturation processes and a wet soil profile explain the observed higher correlations during Event 2.

565 ### 4.1 Landslide and Flood Simulations

In addition to the hydrological simulation, associated hazards such as floods and landslides are also modeled and discussed in this study. The landslides model as described in the previous section

Hydrol. Earth Syst. Sci. Discuss., https://doi.org/10.5194/hess-2018-452
Manuscript under review for journal Hydrol. Earth Syst. Sci.
Discussion started: 25 September 2018


Hydrology and Earth System Sciences
Discussions
Open Access
EGU

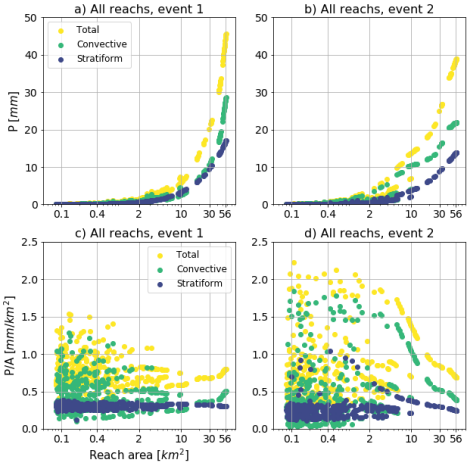


**Figure 12.** Cumulative rainfall versus the area at each reach of the basin for a) Event 1 and b) 2. Panels c) and d) show the average rainfall versus the area at each reach of the basin. Yellow dots correspond to the total, green dots to convective and blue dots to stratiform rainfall. All panels use a logarithmic scale for the basin area.

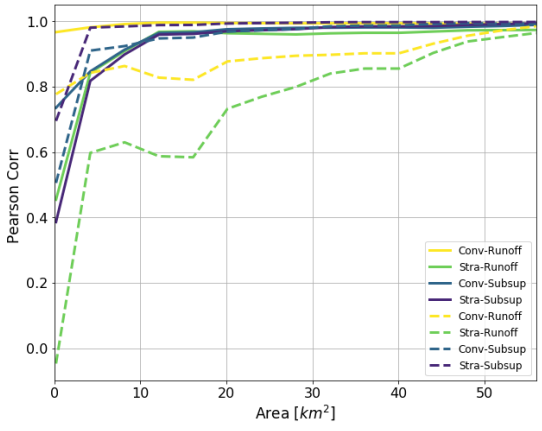


**Figure 13.** Pearson correlations among convective and stratiform portions of the rainfall and runoff and subsurface flow for different reach areas. Dashed lines correspond to Event 1 and continuous lines Event 2.

requires additional information including soil depth $Z$, cohesion $C'$, friction angle $\phi$ and specific weight $\gamma$. According to the description by Osorio (2008), illustrating a clay-slime soil, $C'$ is assumed equal to $4KN$, $\phi$ to $30^0$ and $\gamma$ to 18; $Z$ vary with slope according to Table 1.

Hydrol. Earth Syst. Sci. Discuss., https://doi.org/10.5194/hess-2018-452
Manuscript under review for journal Hydrol. Earth Syst. Sci.
Discussion started: 25 September 2018


Hydrology and Earth System Sciences
Discussions

Figure 14a presents the observed landslides triggered by Event 2 based on aerial photos and satellite images (Landsat/Copernicus, and Google) taken before and after the flash flood. Figure 14b shows, by hills, the map of total unstable cells during the simulation period, and Figure 14c shows the time series of the number of simulated unstable cells during Event 2 (continuous purple line) and the mean rainfall over the basin (inverse axes, blue line). Calibration of the landslide model was performed by finding the maximum overlap between simulated and observed unstable and stable cells, and at the same time reducing the overall number of false positives and false negatives. It is important to note that the calibration strategy is not a cell-by-cell modification of the parameters involved but rather a basin-wide modification of soil properties. A sensitivity analysis of soil parameters is carried out by making small variations of the variables within specified intervals: $\phi$ between 25 and 32, $\gamma$ between 17 and 19, $C'$ between 3.5 and 4.2, and $Z$ between 0.1 and 3 $m$ . The sensitivity analysis suggests that slight variations in the parameter in $Z$ produce significant changes in the modeled landslides, resulting in an overestimation of the number of unstable cells, or no unstable cells at all. Following Table 1, the average soil depth in the basin is only 0.3 m, a value that corresponds to underestimation according to the inspections during field visits. For this reason, the results presented in Figure 14 use a $Z$ map scaled by a calibration factor of 3.5, preserving the spatial dependence on the slope, but achieving a more realistic soil depth and better spatial distribution of landslide occurrence.

The model represents considerably well the spatial distribution of the areas that are prone to trigger shallow landslides during Event 2, showing a significant density of unstable cells in the hills where slides took place. However, despite the calibration efforts, the total number of unstable cells is relatively low compared to observations. A pinpoint localization of the unstable cells is still considered a hard task in part due to the small temporal and spatial scale at which landslide processes take place (Aristizábal et al., 2016; Dhakal and Sidle, 2004; Wu and Sidle, 1995). Additionally, the lack of detailed soil information increases the simulation uncertainty. Notwithstanding the difficulties, the results suggest that the model simulations could have been used and should be used in the future for early detection and warning to improve both short and long-term risk reduction strategies.

According to the model results, a significant portion of the landslides happened during the first of the training convective cores reaching the upper basin (see Figure 14c). Due to the high soil moisture, cells located in the mentioned region where prone to failure. The second and more intense convective core, between 1:20 and 2:15 a.m., also triggered additional slides for an extended period. During storm events, shallow landslides become a significant source of gravels and sediments. These particles tend to reach the river network, increasing the magnitude of the streamflow and its destructive power. Despite this, there is no current explicit link in the model between the landslides scheme and the hydraulic submodel. Nonetheless, HydroFlash assumes that sediment transport is limited by channel capacity, and not by hillslope supply, which in this case is guaranteed by the elevated

Hydrol. Earth Syst. Sci. Discuss., https://doi.org/10.5194/hess-2018-452
Manuscript under review for journal Hydrol. Earth Syst. Sci.
Discussion started: 25 September 2018


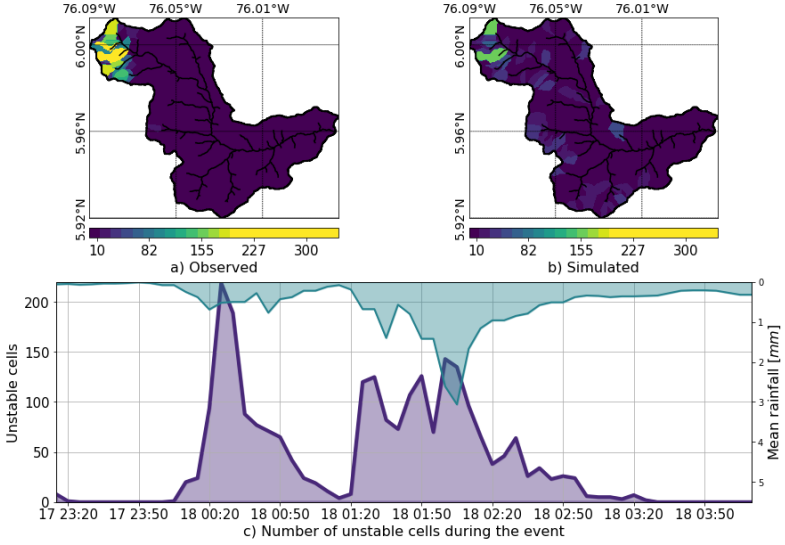


**Figure 14.** a) Observed landslides triggered by Events 1 and 2. The figure is based on aerial photos and satellite images (Landsat/Copernicus, and images available on Google) taken before and after the flash flood event. b) Map of total unstable cells during the simulation period. c) Time series of number of simulated unstable cells during Event 2 (continuous purple line) and mean rainfall over the basin (inverse axes, blue line).

number of landslides.

Figure 15 shows the identification of the flood spots at the peak of Event 2 (May 18th, 2015, 2:00 a.m.) as simulated using HydroFlah. Figures 15b to f present a detail view of the results from the outlet of the basin to the upper region. Cases presented in Figures 15e and f exhibit a satisfactory agreement with observed flood spots (blue shadow). Cases in Figures 15c and d also show a good approximation, but with minor spatial shifts in some sections. The largest spatial differences are observed in Figures 15b. At the entrance of the urban zone, the model overestimates the flood spots. The model results indicate that 11% of flood spots happen at elements of order 1 and 2, and, 18, 38 and 32% happen at orders 3, 4 and 5, respectively. This also highlights a coherent geomorphological representation of the flooded channels and hills with the order.

Hydrol. Earth Syst. Sci. Discuss., https://doi.org/10.5194/hess-2018-452
Manuscript under review for journal Hydrol. Earth Syst. Sci.
Discussion started: 25 September 2018


Hydrology and Earth System Sciences
Discussions
Open Access
EGU

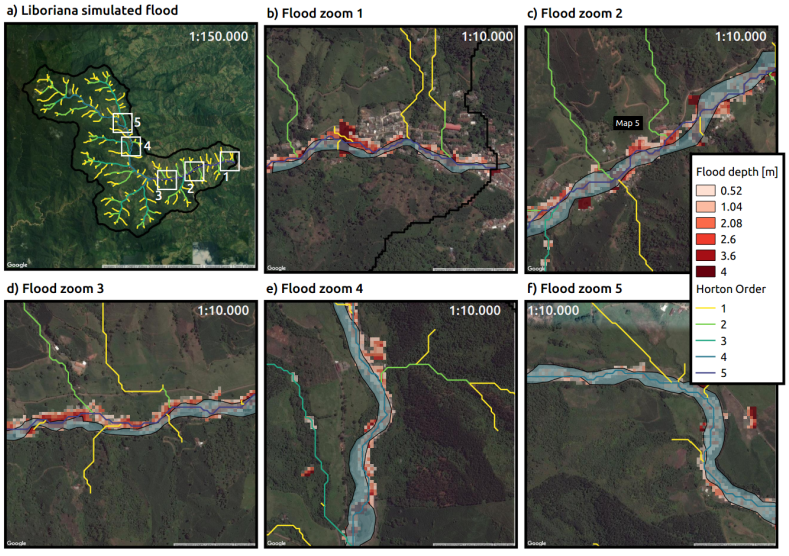


**Figure 15.** Simulated flood spot at the peak of Event 2 in different locations. a) Basin drainage network. White squares correspond to regions of interest highlighted in panes b) to f). b) Zoom at the outlet of the basin, where an important portion of the human and infrastructure loses took place. c) Zoom at La Margarita settlement also affected by the flash flood. d) to f) Zoom at key locations along the principal stream. Observed flood spots are shown in blue polygons and model flood spots in red to white grids.

## 5 Discussion

During the morning of May 18th of 2015, 1:30 a.m local time, a flash flood occurred in the steep La Liboriana basin, in the municipality of Salgar, Department of Antioquia, Colombia, leaving more than 100 human casualties, 535 houses destroyed, and significant infrastructure loses. The disaster was reported to departmental and national authorities around 2:00 and 2:30 a.m. Due to the lack of local information of soil type, land use and real-time hydrometeorological data, La Liboriana case implies a challenge for flash flood prediction, modeling and, consequently, risk management. The present paper introduces a hydrological model-based approach and an integral graphical analysis tool (an integrated spatiotemporal analysis of rainfall evolution, together with soil storages in the basin), not only to simulate and understand all the relevant soil-rainfall-discharge processes that led to the 2015 Salgar flash flood while assessing the associated natural hazards, but also to propose it as a radar QPE-based landslide and flash flood guidance low-cost tool for basins with scarce data and regions with limited resources.

The methodology implies the development of a distributed hydrological model with the capabilities of tracking independently convective and stratiform precipitation within the model as well as

Hydrol. Earth Syst. Sci. Discuss., https://doi.org/10.5194/hess-2018-452
Manuscript under review for journal Hydrol. Earth Syst. Sci.
Discussion started: 25 September 2018




keeping track of the runoff and subsurface portions of the streamflow, coupling a shallow landslide submodel and a one-dimensional flash flood scheme (HydroFlash). The model proposed here indeed allows studying the different hydrological processes relevant to flash flood and landslide occurrence by using different simulation resources, serving as the basis for a better understanding of the overall basin response. This overall approach helps to isolate flood generating mechanisms or causative factors both in time and also in space, focusing on the important physical processes and not only on the statistics (Klemes, 1993; Merz and Blöschl, 2003). It is hoped that knowledge improvement leads to the anticipation of the warning and response by risk management entities.

The evolution of the simulation of Events 1 and 2 show evidence of remarkable behavioral differences. During Event 1 both gravitational and capillary tanks are filled along and across the basin as a result of the quasi-homogeneous rainfall spatial distribution. The return flow is low, and most of the runoff occurs within the first 20 groups (40% of the watershed closest to the outlet). In the period between both events, there is a recession in the capillary and gravitational storages in the entire basin. Capillary storage decays considerably slower than gravitational storage. During Event 2, the flash flood event, the first convective core saturates both capillary and gravitational storages in the upper part of the basin and generates both return flow and significant runoff. Due to soil saturation, the second convective core results mainly in surface runoff. During this event, runoff is generated the lower part of the basin while extreme runoff rates are evident in the upper part of the basin, collocated with the steeper slopes. On the other hand, subsurface flow is more important in magnitude than runoff describing Event 1, while runoff is more relevant for Event 2. The precedent storage and the presence of thunderstorm training profoundly condition the streamflow during Event 2. The overall evidence suggests that precedent capillary moisture in the basin plays an essential role in modulating river discharge. This behavior could be linked to the temporal occurrence and relative importance and timing of stratiform and convective formations previously described.

While convective and stratiform partitioning could influence the runoff and subsurface flow separation, the spatial distribution of rainfall relative to watershed network morphometry structure impose a condition on the hydrological response of the basin. In other words, hydrograph formation is not only determined by the rainfall accumulation or maximum intensity, but also by its spatial structure. The structure of the rainfall associated with La Liboriana event highlights the need to consider in more detail the role of orographic rainfall intensification in practical applications such as early warning systems. Evidence suggests the spatial structure of the rainfall is at least as important as the geomorphological features of the basin regulating the generation of flash flood events.

An integrated spatiotemporal analysis of rainfall evolution, together with soil storages in the basin is necessary to study the relevance of antecedent conditions and precipitation type, intensity, and



location in the generation of flash flood events. Event 1 increased the overall soil moisture with an associated decrease on infiltration rates similar to results reported by Penna et al. (2011) and Zehe et al. (2010), low infiltration increase runoff rates, which finally affects the susceptibility of the basin to flash floods occurrence (Wagner et al., 1999; Penna et al., 2011; Tramblay et al., 2012). La Liboriana geomorphological characteristics, corresponding to a steep tropical basin, determine the potential energy that controls water transit velocity. Water tends to reach faster the channels in order 1 and 2 hills, and, at the same time, the sediment production and transport in these hills tend to be larger. Order 3 sub-basins most likely act as transport elements, with no important energy losses. Floods tend to occur in order 4 and 5 sub-basins due to the widening of the channel and slope attenuation.

Different authors have focused on trying to understand the general causative factors behind the occurrence of flash floods finding similar to our results, a significant role of basing geomorphology, orography and local convection. For example, Lehmann and Or (2012), using a shallow landslide model, finds an important role of the topography and the rainfall conditions. Turkington et al. (2014) shows how intense locally driven convection appears to be the main meteorological trigger for flash occurrence in the French Alpes.Camarasa-Belmonte (2016) shows how rainfall intensity and duration influences the shape of the hydrograph, with intense rainfall shortening the response time of the basin, and large durations increasing the flood peak. In the Mediterranean region, Boudou et al. (2016) states that in addition to the rainfall, geomorphological characteristics and antecedent soil conditions are key in the generation of flash flooding.

However useful, the evidence in this work only takes into account two successive events; an analysis of more cases and different spatial scales (different basins) would provide robust conclusions in this direction. It is clear that it is not conclusive enough to focus on a single extreme event, rather than on a spectrum of floods Merz and Blöschl (2003). The results suggest it is imperative to study in depth the long-term link between the relative basin and drainage network orientation and the preferred path of precipitation events and its role in defining the frequency of flash flood occurrence. A better understanding of the network-hills-preferential rainfall advection structure could provide information about basins prone to flash floods when information is scarce.

## 6 Conclusions

Extreme rainfall events such as the one that triggered La Liboriana tragedy frequently take place in Colombia and the entire global tropical belt over ungauged basins, often triggering flash floods and torrential flows, endangering vulnerable communities due to poor long-term planning and lack of



functional early warning systems. There is a global need for better knowledge and understanding of the hydrological and meteorological conditions that, combined, lead to the manifestation of natural hazards. Such understanding must result in useful practical applications that improve risk management practices saving lives.

In the case of La Liboriana flash flood, radar reflectivity fields were available from a C-Band radar operated by the Early Warning System of Medellín and its metropolitan area as part of a local risk management strategy. While the municipality of Salgar is located far outside Medellín's metropolitan area, the radar is about 60 km away from Salgar, and the reflectivity retrievals enable the classification of precipitation fields into convective and stratiform areas using widely accepted methodologies by the meteorological community. Radar reflectivity is also a proxy for precipitation allowing a quantitative estimation. This estimation was used together with the hydrological modeling to assess the different basin-wide processes taking place during the flash flood triggering rainfall event.

The overall methodology reproduces considerably well the magnitude and timing of La Liboriana flash flood discharge peak, as well as the areas of regional land-slide occurrence and flood spots location. Simulation results indicate that the flash-flood and the regional land-slide features were strongly influenced by the antecedent rainfall associated with a northeasterly stratiform event that recharged the gravitational and capillary storages. The hydrologic simulation shows that the antecedent event set wet conditions in the entire basin before the occurrence of the flash flood event, governing the streamflow during the latter. The first of the two successive convective cores (thunderstorm training) over the same region during the flash flood event saturated both capillary and gravitational storages in the upper part of the basin and generated both return flow and significant runoff. The second convective core resulted mainly in surface runoff spatially collocated with the steeper slopes, generating the kinetic energy needed to produce La Liboriana flash flood. Overall results also show an excellent agreement between the simulated flood spots and the observed ones; this in spite of the limitations imposed by the resolution of the DEM used for extracting cross sections, and the model simplifications described in the Methodology section.

The described model-based approach is useful to isolate flood generating mechanisms and as a tool for policy-makers not only for short-term decisions in the context of an early warning system but also as a planning resource for long-term risk management. While several improvements could be implemented, including a better representation of hydraulic parameters, and a link between landslides and flood spots similar to the strategy in the STEP-TRAMM model (Fan et al., 2017), the results suggest it is possible to use the low-cost methodology introduced here to not only improve our understanding of hydrological processes but also as a risk management tool in countries and re-



gions with scarce resources. In the case of Salgar, there was radar information available, but in many cases, the only near-real-time precipitation information comes from satellite retrievals. It would be very useful from a practical point of view to assess in which cases satellite information is enough for risk management applications. Comparing the Salgar case with the Mocoa (Department of Putumayo, Colombia) April 1st, 2017 flash flood that resulted in more than 330 fatalities could help address this question.

## 7 Acknowledgements

This work was supported by SIATA (Sistema de Alerta Temprana de Medellín y el Valle de Aburrá) funds provided by Area Metropolitana de Medellín y del Valle de Aburrá (AMVA), Municipio de Medellín, Grupo EPM, and ISAGEN under the Research and Technology Contract CD511 of 2017. Nicolás Velásquez was partly funded by Universidad Nacional de Colombia under the Facultad de Minas graduate scholarship program.

Hydrol. Earth Syst. Sci. Discuss., https://doi.org/10.5194/hess-2018-452
Manuscript under review for journal Hydrol. Earth Syst. Sci.
Discussion started: 25 September 2018


Hydrology and Earth System Sciences
Discussions

## References

760 Adamovic, M., Branger, F., Braud, I., and Kralisch, S.: Development of a data-driven semi-distributed hydrological model for regional scale catchments prone to Mediterranean flash floods, Journal of Hydrology, 541, 173–189, doi:10.1016/j.jhydrol.2016.03.032, http://dx.doi.org/10.1016/j.jhydrol.2016.03.032, 2016.

Aristizábal, E., Vélez, J. I., Martínez, H. E., and Jaboyedoff, M.: SHIA_Landslide: a distributed conceptual and physically based model to forecast the temporal and spatial occurrence of shallow landslides triggered 765 by rainfall in tropical and mountainous basins, Landslides, 13, 497–517, doi:10.1007/s10346-015-0580-7, 2016.

Aronica, G. T., Brigandí, G., and Morey, N.: Flash floods and debris flow in the city area of Messina, northeast part of Sicily, Italy in October 2009: The case of the Giampilieri catchment, Natural Hazards and Earth System Science, 12, 1295–1309, doi:10.5194/nhess-12-1295-2012, 2012.

770 ASF, J.: Dataset: ASF DAAC 2015, ALOS PALSAR Radiometric Terrain Corrected high res; Includes Material JAXA/METI 2007, doi:10.5067/Z97HFCNKR6VA, https://vertex.daac.asf.alaska.edu/, 2011.

Ayalew, T. B., Krajewski, W. F., and Mantilla, R.: Connecting the power-law scaling structure of peak-discharges to spatially variable rainfall and catchment physical properties, Advances in Water Resources, 71, 32–43, doi:10.1016/j.advwatres.2014.05.009, http://dx.doi.org/10.1016/j.advwatres.2014.05.009, 2014.

775 Berne, A. and Krajewski, W.: Radar for hydrology: Unfulfilled promise or unrecognized potential?, Advances in Water Resources, 51, 357 – 366, doi:https://doi.org/10.1016/j.advwatres.2012.05.005, http://www.sciencedirect.com/science/article/pii/S0309170812001157, 35th Year Anniversary Issue, 2013.

Beven, K.: Kinematic subsurface stormflow, Water Resources Research, 17, 1419–1424, doi:10.1029/WR017i005p01419, 1981.

780 Beven, K.: Towards integrated environmental models of everywhere: uncertainty, data and modelling as a learning process, Hydrology and Earth System Sciences, 11, 460–467, doi:10.5194/hess-11-460-2007, http://www.hydrol-earth-syst-sci.net/11/460/2007/{%}5Cnhttps://hal.archives-ouvertes.fr/hal-00305631/, 2007.

Blöschl, G., Sivapalan, M., Wagener, T., Viglione, A., and Savenije, H.: Runoff Prediction in Ungauged Basins, in: Runoff Prediction in Ungauged Basins: Synthesis across Processes, Places and Scales, 785 edited by Blöschl, G., Sivapalan, M., Wagener, T., Viglione, A., and Savenije, H., Cambridge University Press, Cambridge, https://www.cambridge.org/core/books/runoff-prediction-in-ungauged-basins/runoff-prediction-in-ungauged-basins/A5DFE99C3CA857127C4C03C6C20032EE, 2012.

Bonell, M., McDonnell, J. J., Scatena, F. N., Seibert, J., Uhlenbrook, S., and van Lanen, H. A. J.: HELPing FRIENDs in PUBs: Charting a course for synergies within international water research programmes in 790 gauged and ungauged basins, Hydrological Processes, 20, 1867–1874, doi:10.1002/hyp.6196, 2006.

Borga, M., Anagnostou, E. N., Blöschl, G., and Creutin, J. D.: Flash flood forecasting, warning and risk management: The HYDRATE project, Environmental Science and Policy, 14, 834–844, doi:10.1016/j.envsci.2011.05.017, 2011.

Borga, M., Stoffel, M., Marchi, L., Marra, F., and Jakob, M.: Hydrogeomorphic response to extreme 795 rainfall in headwater systems: Flash floods and debris flows, Journal of Hydrology, 518, 194–205, doi:10.1016/j.jhydrol.2014.05.022, http://dx.doi.org/10.1016/j.jhydrol.2014.05.022, 2014.



Boudou, M., Lang, M., Vinet, F., and C??ur, D.: Comparative hazard analysis of processes leading to remarkable flash floods (France, 1930???1999), Journal of Hydrology, 541, 533–552, doi:10.1016/j.jhydrol.2016.05.032, http://dx.doi.org/10.1016/j.jhydrol.2016.05.032, 2016.

Braud, I., Borga, M., Gourley, J., H??rlimann, M., Zappa, M., and Gallart, F.: Flash floods, hydro-geomorphic response and risk management, Journal of Hydrology, 541, 1–5, doi:10.1016/j.jhydrol.2016.08.005, http://dx.doi.org/10.1016/j.jhydrol.2016.08.005, 2016.

Camarasa-Belmonte, A. M.: Flash floods in Mediterranean ephemeral streams in Valencia Region (Spain), Journal of Hydrology, doi:10.1016/j.jhydrol.2016.03.019, 2016.

Castillo, V. M., Gómez-Plaza, A., and Martínez-Mena, M.: The role of antecedent soil water content in the runoff response of semiarid catchments: A simulation approach, Journal of Hydrology, 284, 114–130, doi:10.1016/S0022-1694(03)00264-6, 2003.

Cea, L. and Blade, E.: A simple and efficient unstructured finite volume scheme for solving the shallow water equations in overland flow applications, Water Resources Research, 51, 5464–5486, doi:10.1002/2014WR016259, 2015.

Creutin, J. D. and Borga, M.: Radar hydrology modifies the monitoring of flash-flood hazard, Hydrological Processes, 17, 1453–1456, doi:10.1002/hyp.5122, 2003a.

Creutin, J. D. and Borga, M.: Radar hydrology modifies the monitoring of flash-flood hazard, Hydrological Processes, 17, 1453–1456, doi:10.1002/hyp.5122, 2003b.

Dhakal, A. S. and Sidle, R. C.: Distributed simulations of landslides for different rainfall conditions, Hydrological Processes, 18, 757–776, doi:10.1002/hyp.1365, 2004.

Douinot, A., Roux, H., Garambois, P. A., Larnier, K., Labat, D., and Dartus, D.: Accounting for rainfall systematic spatial variability in flash flood forecasting, Journal of Hydrology, 541, 359–370, doi:10.1016/j.jhydrol.2015.08.024, http://dx.doi.org/10.1016/j.jhydrol.2015.08.024, 2016.

Duan, Q., Schaake, J., Andreassian, V., Franks, S., Goteti, G., Gupta, H., Gusev, Y., Habets, F., Hall, a., Hay, L., Hogue, T., Huang, M., Leavesley, G., Liang, X., Nasonova, O., Noilhan, J., Oudin, L., Sorooshian, S., Wagener, T., and Wood, E.: Model Parameter Estimation Experiment (MOPEX): An overview of science strategy and major results from the second and third workshops, Journal of Hydrology, 320, 3–17, doi:10.1016/j.jhydrol.2005.07.031, 2006.

(eds.), D. C. A. D. I.: Severe Convective Storms, Meteorological Monographs, American Meteorological Society, http://gen.lib.rus.ec/book/index.php?md5=7AEF0E8299AB41644901046180BED4FC, 2001.

Fan, L., Lehmann, P., McArdell, B., and Or, D.: Linking rainfall-induced landslides with debris flows runout patterns towards catchment scale hazard assessment, Geomorphology, 280, 1–15, doi:10.1016/j.geomorph.2016.10.007, http://dx.doi.org/10.1016/j.geomorph.2016.10.007, 2017.

Foster G.R., Huggins L.F., M. L.: A Laboratory Study of Rill Hydraulics: I. Velocity Relationships, American Society of Agricultural and Biological Engineers, 3, 0790–0796, doi:10.13031/2013.32873, 1984.

Fragoso, M., Trigo, R. M., Pinto, J. G., Lopes, S., Lopes, a., Ulbrich, S., and Magro, C.: The 20 February 2010 Madeira flash-floods: Synoptic analysis and extreme rainfall assessment, Natural Hazards and Earth System Science, 12, 715–730, doi:10.5194/nhess-12-715-2012, 2012.

Francés, F., Vélez, J. I., and Vélez, J. J.: Split-parameter structure for the automatic calibration of distributed hydrological models, Journal of Hydrology, 332, 226–240, doi:10.1016/j.jhydrol.2006.06.032, 2007.



Garambois, P. a., Roux, H., Larnier, K., Castaings, W., and Dartus, D.: Characterization of process-oriented hydrologic model behavior with temporal sensitivity analysis for flash floods in Mediterranean catchments, Hydrology and Earth System Sciences, 17, 2305–2322, doi:10.5194/hess-17-2305-2013, 2013.

Gibson, S., Park, H. J., and Fleming, M.: Modeling Watershed and Riverine Sediment Processes with HEC-HMS and HEC-RAS, Watershed Management, pp. 1340–1349, 2010.

Gochis, D., Schumacher, R., Friedrich, K., Doesken, N., Kelsch, M., Sun, J., Ikeda, K., Lindsey, D., Wood, A., Dolan, B., Matrosov, S., Newman, A., Mahoney, K., Rutledge, S., Johnson, R., Kucera, P., Kennedy, P., Sempere-Torres, D., Steiner, M., Roberts, R., Wilson, J., Yu, W., Chandrasekar, V., Rasmussen, R., Anderson, A., and Brown, B.: The great Colorado flood of September 2013, Bulletin of the American Meteorological Society, 96, 1461–1487, doi:10.1175/BAMS-D-13-00241.1, 2015.

Gruntfest, E. and Handmer, J.: Coping with Flash Floods, NATO science series. Partnership sub-series 2, Environmental security, Springer Netherlands, https://books.google.com.co/books?id=pwsczTbbY9sC, 2001.

Hardy, J., Gourley, J. J., Kirstetter, P. E., Hong, Y., Kong, F., and Flamig, Z. L.: A method for probabilistic flash flood forecasting, Journal of Hydrology, 541, 480–494, doi:10.1016/j.jhydrol.2016.04.007, http://dx.doi.org/10.1016/j.jhydrol.2016.04.007, 2016.

Houze, R.: Mesoscale convective systems, Reviews of Geophysics, 42, doi:10.1029/2004RG000150, https://agupubs.onlinelibrary.wiley.com/doi/abs/10.1029/2004RG000150, 2004.

Houze, R. A.: Observed structure of mesoscale convective systems and implications for large-scale heating, Quarterly Journal of the Royal Meteorological Society, 115, 425–461, doi:10.1002/qj.49711548702, 1989.

Houze, R. A., Rasmussen, K. L., Zuluaga, M. D., and Brodzik, S. R.: The variable nature of convection in the tropics and subtropics: A legacy of 16 years of the Tropical Rainfall Measuring Mission satellite, Reviews of Geophysics, 53, 994–1021, doi:10.1002/2015RG000488, 2015.

Jonkman, S.: Global perspectives on loss of human life caused by floods, NATURAL HAZARDS, 34, 151–175, doi:10.1007/s11069-004-8891-3, 2005.

Kahana, R., Ziv, B., Enzel, Y., and Dayan, U.: Synoptic climatology of major floods in the Negev Desert, Israel, International Journal of Climatology, 22, 867–882, doi:10.1002/joc.766, 2002.

Kirkby, M. J. and Chorley, R. J.: Throughflow, Overland Flow and Erosion, International Association of Scientific Hydrology. Bulletin, 12, 5–21, doi:10.1080/02626666709493533, http://www.tandfonline.com/doi/abs/10.1080/02626666709493533, 1967.

Klemes, V.: Probability of extreme hydrometeorological events—A differ- ent approach, in Extreme Hydrological Events: Precipitation, Floods and Droughts, IAHS Publ, 1993.

Kubota, J. and Sivapalan, M.: Towards a Catchment-Scale Model of Subsurface Small-Scale Process-Based Modelling and Runoff Generation Based on Synthesis of Field Studies, Hydrological Processes, 9, 541–554, 1995.

Lehmann, P. and Or, D.: Hydromechanical triggering of landslides: From progressive local failures to mass release, Water Resources Research, 48, 1–24, doi:10.1029/2011WR010947, 2012.

Leopold, L.B., M. T.: The hydraulic geometry of stream channels and some physiographic implications, Geological survey professional paper, 1953.



Llasat, M. C., Marcos, R., Turco, M., Gilabert, J., and Llasat-Botija, M.: Trends in flash flood events versus convective precipitation in the Mediterranean region: The case of Catalonia, Journal of Hydrology, 541, 24–37, doi:10.1016/j.jhydrol.2016.05.040, http://dx.doi.org/10.1016/j.jhydrol.2016.05.040, 2016.

Mapes, B., Warner, T., Xu, M., and Negri, A. J.: Diurnal Patterns of Rainfall in Northwestern South America. Part I: Observations and Context, Monthly Weather Review, 131, 799–812, doi:10.1175/1520-0493(2003)131<0799:DPORIN>2.0.CO;2, https://doi.org/10.1175/1520-0493(2003)131<0799:DPORIN>2.0.CO;2, 2003.

Marra, F., Destro, E., Nikolopoulos, E. I., Zoccatelli, D., Dominique Creutin, J., Guzzetti, F., and Borga, M.: Impact of rainfall spatial aggregation on the identification of debris flow occurrence thresholds, Hydrology and Earth System Sciences, 21, 4525–4532, doi:10.5194/hess-21-4525-2017, 2017.

Merz, R. and Blöschl, G.: A process typology of regional floods, Water Resources Research, 39, 1–20, doi:10.1029/2002WR001952, http://doi.wiley.com/10.1029/2002WR001952, 2003.

Norbiato, D., Borga, M., Degli Esposti, S., Gaume, E., and Anquetin, S.: Flash flood warning based on rainfall thresholds and soil moisture conditions: An assessment for gauged and ungauged basins, Journal of Hydrology, pp. 274–290, doi:10.1016/j.jhydrol.2008.08.023, 2008.

Osorio, H.G., A. S.: Unidades de suelo representativas de la zona cafetera de Colombia, Federación de Cafeteros de Colombia, 2008.

Penna, D., Tromp-Van Meerveld, H. J., Gobbi, a., Borga, M., and Dalla Fontana, G.: The influence of soil moisture on threshold runoff generation processes in an alpine headwater catchment, Hydrology and Earth System Sciences, 15, 689–702, doi:10.5194/hess-15-689-2011, 2011.

Peterson, P.: F2PY: a tool for connecting Fortran and Python programs, International Journal of Computational Science and Engineering, 4, 296, doi:10.1504/IJCSE.2009.029165, http://www.inderscience.com/link.php?id=29165, 2009.

Piper, D., Kunz, M., Ehmele, F., Mohr, S., Mühr, B., Kron, A., and Daniell, J.: Exceptional sequence of severe thunderstorms and related flash floods in May and June 2016 in Germany. Part I: Meteorological background, Natural Hazards and Earth System Sciences Discussions, pp. 1–30, doi:10.5194/nhess-2016-275, http://www.nat-hazards-earth-syst-sci-discuss.net/nhess-2016-275/, 2016.

Poveda, G. and Mesa, O. J.: On the existence of Lloró (the rainiest locality on Earth): Enhanced ocean-land-atmosphere interaction by a low-level jet, Geophysical Research Letters, 27, 1675–1678, doi:10.1029/1999GL006091, https://agupubs.onlinelibrary.wiley.com/doi/abs/10.1029/1999GL006091, 2000.

Poveda, G., Vélez, J. I., Mesa, O. J., Cuartas, A., Barco, J., Mantilla, R. I., Mejía, J. F., Hoyos, C. D., Ramírez, J. M., Ceballos, L. I., Zuluaga, M. D., Arias, P. a., Botero, B. a., Montoya, M. I., Giraldo, J. D., and Quevedo, D. I.: Linking Long-Term Water Balances and Statistical Scaling to Estimate River Flows along the Drainage Network of Colombia, Journal of Hydrologic Engineering, 12, 4–13, doi:10.1061/(ASCE)1084-0699(2007)12:1(4), 2007.

Rennó, C. D., Nobre, A. D., Cuartas, L. A., Soares, J. V., Hodnett, M. G., Tomasella, J., and Waterloo, M. J.: HAND, a new terrain descriptor using SRTM-DEM: Mapping terra-firme rainforest environments in Amazonia, Remote Sensing of Environment, 112, 3469–3481, doi:10.1016/j.rse.2008.03.018, http://linkinghub.elsevier.com/retrieve/pii/S003442570800120X, 2008.



915 Rodriguez-Blanco, M., Taboada-Castro, M., and Taboada-Castro, M.: Rainfall–runoff response and event-based runoff coefficients in a humid area (northwest Spain), Hydrological Sciences Journal, 403, 319–329, doi:10.1080/02626669509491418, http://www.tandfonline.com/action/journalInformation?journalCode=thsj20{%}0Ahttp://www.tandfonline.com/action/journalInformation?journalCode=thsj20, 2012.

Roux, H., Labat, D., Garambois, P. A., Maubourguet, M. M., Chorda, J., and Dartus, D.: A physically-based 920 parsimonious hydrological model for flash floods in Mediterranean catchments, Natural Hazards and Earth System Science, 11, 2567–2582, doi:10.5194/nhess-11-2567-2011, 2011.

Ruiz-Villanueva, V., Díez-Herrero, A., Bodoque, J. M., Ballesteros Cánovas, J. A., and Stoffel, M.: Characterisation of flash floods in small ungauged mountain basins of Central Spain using an integrated approach, Catena, 110, 32–43, doi:10.1016/j.catena.2013.06.015, http://dx.doi.org/10.1016/j.catena.2013.06.925 015, 2013.

Šálek, M., Brezková, L., and Novák, P.: The use of radar in hydrological modeling in the Czech Republic – case studies of flash floods, Natural Hazards and Earth System Science, 6, 229–236, doi:10.5194/nhess-6-229-2006, 2006.

Schumacher, R. S. and Johnson, R. H.: Organization and Environmental Properties of Extreme-Rain-Producing 930 Mesoscale Convective Systems, Monthly Weather Review, 133, 961–976, doi:10.1175/MWR2899.1, http://journals.ametsoc.org/doi/abs/10.1175/MWR2899.1, 2005.

Seibert, J. and Beven, K. J.: Gauging the ungauged basin : how many discharge measurements are needed?, Hydrology and Earth System Sciences, 13, 883–892, doi:10.5194/hessd-6-2275-2009, http://www.hydrol-earth-syst-sci.net/13/883/2009/, 2009.

935 Shope, C. L.: Disentangling event-scale hydrologic flow partitioning in mountains of the Korean Peninsula under extreme precipitation, Journal of Hydrology, 538, 399–415, doi:10.1016/j.jhydrol.2016.04.050, http://dx.doi.org/10.1016/j.jhydrol.2016.04.050, 2016.

Sidle, R., Gomi, T., and Tsukamoto, Y.: Discovery of zero-order basins as an important link for progress in hydrogeomorphology, Hydrological Processes, pp. 1–7, doi:10.1002/hyp.13246, http://doi.wiley.com/10.1002/940 hyp.13246, 2018.

Sivapalan, M., Takeuchi, K., FRANKS, S. W., GUPTA, V. K., KARAMBIRI, H., LAKSHMI, V., LIANG, X., McDONNELL, J. J., MENDIONDO, E. M., J, P. E. O., OKI, T., POMEROY, J. W., SCHERTZER, D., UHLENBROOK, S., and E. ZEHE: IAHS Decade on Predictions in Ungauged Basins (PUB), 2003–2012: Shaping an exciting future for the hydrological sciences, Hydrological 945 Sciences Journal, pp. 857–880, doi:10.1080/02626667.2015.1131899, http://www.tandfonline.com/action/journalInformation?journalCode=thsj20{%}5Cnhttp://dx.doi.org/10.1080/02626667.2015.1131899, 2016.

Steiner, M., Houze, R. a., and Yuter, S. E.: Climatological Characterization of Three-Dimensional Storm Structure from Operational Radar and Rain Gauge Data, doi:10.1175/1520-0450(1995)034<1978:CCOTDS>2.0.CO;2, papers3://publication/uuid/950 D11C9905-6CE2-40B5-8A93-5E5300EB3A6E, 1995.

Takahashi, T.: Debris flow, Taylor y francis, 2 edn., 1991.

Tramblay, Y., Bouaicha, R., Brocca, L., Dorigo, W., Bouvier, C., Camici, S., and Servat, E.: Estimation of antecedent wetness conditions for flood modelling in northern Morocco, Hydrology and Earth System Sciences, 16, 4375–4386, doi:10.5194/hess-16-4375-2012, 2012.



Turkington, T., Ettema, J., Van Westen, C. J., and Breinl, K.: Empirical atmospheric thresholds for debris flows and flash floods in the southern French Alps, Natural Hazards and Earth System Sciences, 14, 1517–1530, doi:10.5194/nhess-14-1517-2014, 2014.

Vannier, O., Anquetin, S., and Braud, I.: Investigating the role of geology in the hydrological response of Mediterranean catchments prone to flash-floods: Regional modelling study and process understanding, Journal of Hydrology, 541, 158–172, doi:10.1016/j.jhydrol.2016.04.001, http://dx.doi.org/10.1016/j.jhydrol.2016.04.001, 2016.

Vélez, J.: Desarrollo de un modelo hidrológico conceptual y distribuido orientado a la simulación de crecidas, Tesis doctoral - Universidad Politécnica de Valencia, p. 266, 2001.

Wagener, T., Gupta, H., Yatheendradas, S., Goodrich, D., Unkrich, C., and Schaffner, M.: Understanding sources of uncertainty in flash-flood forecasting for semi-arid regions., IAHS Publication 313, pp. 204–212, 2007.

Wagner, W., Lemoine, G., and Rott, H.: A method for estimating soil moisture from ERS Scatterometer and soil data, Remote Sensing of Environment, 70, 191–207, doi:10.1016/S0034-4257(99)00036-X, 1999.

Wu, W. and Sidle, R. C.: and Number Values Agreed Closely With, Water Resources, 31, 2097–2110, doi:10.1029/95WR01136, 1995.

Yamanaka, T. and Ma, W.: Runoff prediction in a poorly gauged basin using isotope-calibrated models, Journal of Hydrology, 544, 567–574, doi:10.1016/j.jhydrol.2016.12.005, http://dx.doi.org/10.1016/j.jhydrol.2016.12.005, 2017.

Yatheendradas, S., Wagener, T., Gupta, H., Unkrich, C., Goodrich, D., Schaffner, M., and Stewart, A.: Understanding uncertainty in distributed flash flood forecasting for semiarid regions, Water Resources Research, 44, 1–17, doi:10.1029/2007WR005940, 2008.

Younis, J., Anquetin, S., and Thielen, J.: The benefit of high-resolution operational weather forecasts for flash flood warning, Hydrology and Earth System Sciences Discussions, 5, 345–377, doi:10.5194/hessd-5-345-2008, 2008.

Zehe, E., Graeff, T., Morgner, M., Bauer, A., and Bronstert, A.: Plot and field scale soil moisture dynamics and subsurface wetness control on runoff generation in a headwater in the Ore Mountains, Hydrology and Earth System Sciences, 14, 873–889, doi:10.5194/hess-14-873-2010, 2010.